TMEDA in IronCatalyzed Hydromagnesiation: Formation of Iron(II)Alkyl Species for Controlled Reduction to AlkeneStabilized Iron(0)

RESEARCH ARTICLE

TMEDA in Iron-Catalyzed Hydromagnesiation: Formation of Iron(II)-Alkyl Species for Controlled Reduction to Alkene-Stabilized Iron(0)

Peter G. N. Neate,[a] Mark D. Greenhalgh,[b] William W. Brennessel,[a] Stephen P. Thomas*[c] and Michael L. Neidig*[a]

Abstract: *N,N,N',N'*-Tetramethylethylenediamine (TMEDA) has been one of the most prevalent and successful additives used in iron catalysis, finding application in reactions as diverse as cross-coupling, C-H activation and borylation. However, the role that TMEDA plays in these reactions remains largely undefined. Herein, studying the iron-catalyzed hydromagnesiation of styrene derivatives using TMEDA has provided molecular-level insight into the role of TMEDA in achieving effective catalysis. Key is the initial formation of TMEDA-iron(II) alkyl species which undergo a controlled reduction to selectively form catalytically active styrene-stabilized iron(0)-alkyl complexes. While TMEDA is not bound to the catalytically active species, these active iron(0) complexes cannot be accessed in the absence of TMEDA. This mode of action, allowing for controlled reduction and access to iron(0) species, represents a new paradigm for the role of this important reaction additive in iron catalysis.

Introduction

Iron catalysis has seen significant development due to the increasing need for sustainable chemical synthesis.[1–12] As one of the most prevalent additives used in iron catalysis, *N,N,N',N'*-tetramethylethylenediamine (TMEDA) has enabled a wide variety of reactions to be achieved with high conversion and selectivity. Iron-catalyzed cross-coupling has been an area where TMEDA has been applied with particular success. Cross-coupling of a range of organometallic reagents with halides and pseudo-halides has been applied to achieve C(sp^2)-C(sp^3) and even C(sp^3)-C(sp^3) bond formation (Scheme 1 A).[13–22] Notable examples include the reductive coupling of aryl bromides with alkyl or alkenyl halides;[17,18] difluoroalkylation;[22] and release-capture ethylene coupling.[21] Additionally, the use of TMEDA as an additive extends well beyond cross-coupling, having proved essential for reactions including Miyaura-type borylation of alkyl electrophiles, C-H alkylation and the hydromagnesiation of styrene derivatives (Scheme 1 B-D).[23–27]

Despite being a crucial component of many reactions, the role that TMEDA plays in achieving effective catalysis within such reactions is largely undefined. Attempts to ascertain its function within iron-catalyzed cross-coupling reactions have been a particular focus, with Bedford and co-workers having carried out perhaps the most extensive investigations.[28–31] However, a definitive role has yet to be established. Early work by Nagashima and co-workers suggested that TMEDA coordinates the iron center, with productive reactivity taking place from the bis-transmetallated complex;[28] Bedford and co-workers later showed that this TMEDA-bound species did not react at a rate consistent with the catalytic reaction. They proposed that the tris-mesityl iron(II) ate complex was responsible for catalysis, with TMEDA acting as a "chaperone" to stabilize off-cycle species prior to their re-entry into the primary catalytic cycle.[29,31]

Despite the widespread use of TMEDA outside the realm of cross-coupling, its effects have yet to be investigated in other reactions, such as the iron-catalyzed hydromagnesiation of

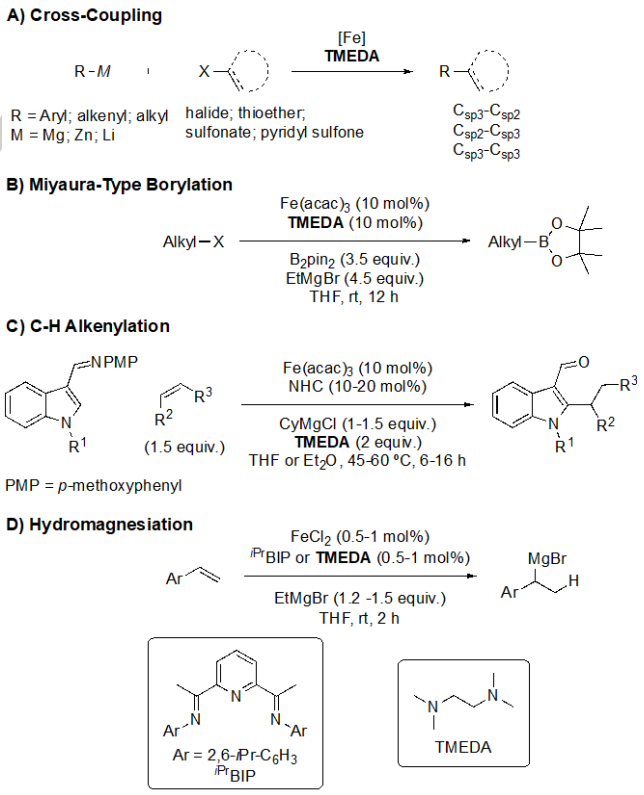

Scheme 1. Examples of iron-catalyzed reactions that use TMEDA as an additive.

[*] Dr. P. G. N. Neate, Dr. W. W. Brennessel, Prof. Dr. M. L. Neidig
Department of Chemistry, University of Rochester, B31 Hutchison Hall
120 Trustee Road, Rochester, NY 14627 (USA)
E-mail: neidig@chem.rochester.edu

Dr. M. D. Greenhalgh
Department of Chemistry, University of Warwick
Coventry, CV4 7AL (UK)
E-Mail: mark.greenhalgh@warwick.ac.uk

Dr. S. P. Thomas
EaStCHEM School of Chemistry, University of Edinburgh, Joseph Black Building
David Brewster Road, Edinburgh, UK, EH9 3FJ (UK)
E-mail: stephen.thomas@ed.ac.uk

Supporting information for this article is given via a link at the end of the document.

styrene derivatives. As a modular platform for generating molecular complexity, iron-catalyzed hydromagnesiation can generate a wealth of formal hydrofunctionalization products in high yield and with control of regio- and stereoselectivity.[26,27,32] In this reaction, TMEDA can be used in loadings as low as 1 equivalent with respect to iron, contrary to several other reactions where TMEDA is used as an additive. However, its presence is still imperative for reactivity, with trace product formation in its absence with iron salts alone. Additionally, the iron-catalyzed hydromagnesiation of styrene derivatives was initially reported using the electronically non-innocent bis(imino)pyridine (BIP) ligand (Scheme 1 D).[32] Our subsequent mechanistic study of this catalytic system revealed a formal iron(0) complex, $[BIPFe(Et)(CH_2{=}CH_2)]^-$, as the catalyst resting state.[33] This raises the question of how TMEDA allows access to the same reactivity as an electronically non-innocent ligand. Altogether, this made the iron-catalyzed hydromagnesiation of styrene derivatives, with TMEDA, an ideal platform to examine how this versatile additive exerts its vital influence. Through the use of time-resolved, freeze-trapped ^{57}Fe Mössbauer spectroscopy and independent synthesis and characterization of key intermediates, molecular-level definition of the role of TMEDA in achieving effective catalysis is reported herein.

Results and Discussion

Effect of TMEDA Loading on Catalytic Performance

As the loading of TMEDA used in reactions varies significantly, from catalytic to stoichiometric quantities, our initial studies examined the effect of changing the loading of TMEDA on the iron-catalyzed hydromagnesiation of 2-methoxystyrene (Figure 1).

In the absence of TMEDA, using $FeCl_2$ alone (1 mol%), negligible reactivity was observed (<5% yield after 1 hour). Addition of TMEDA enhanced reactivity, with increases in the loading from 0.5-2 mol% proving beneficial to both the rate and sustained catalytic activity. However, a large excess of TMEDA (10 mol%) resulted in a significantly longer induction period alongside the sustained catalytic performance. The absence of a clear stoichiometric relationship between $FeCl_2$ and TMEDA suggests that it may not be bound to the iron center within the principal catalytic cycle. However, paramount to understanding the origin of these effects was determining the *in situ* iron speciation by direct spectroscopic means.

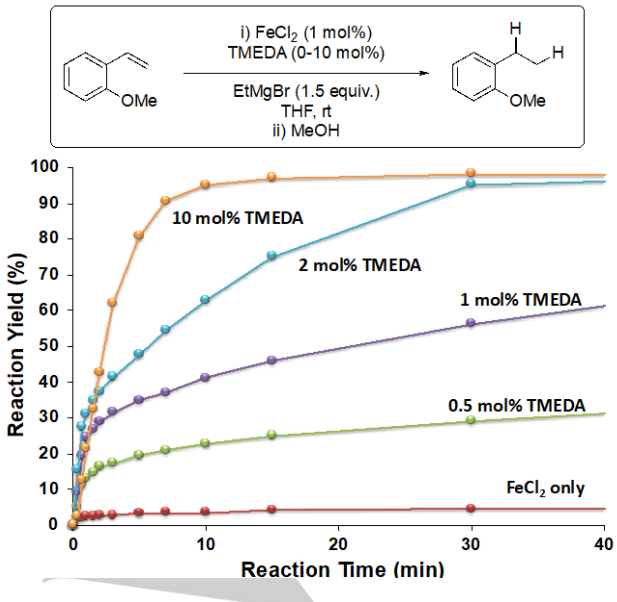

Figure 1. Kinetic profile of the hydromagnesiation of 2-methoxystyrene with various equivalents of TMEDA.

In Situ Iron Speciation on Reaction with Grignard Reagent

In order to build up a picture of iron species accessible in this reaction, it was first important to assess stoichiometric reactions with EtMgBr to identify what species may initially be formed. These reactions were carried out at reduced temperatures to stabilize any species accessed. The speciation resulting from reaction of $^{57}FeCl_2$ with EtMgBr, in the presence of TMEDA (2 equiv.) was examined by freeze-quenching samples in liquid nitrogen for Mössbauer spectroscopy. Reaction with 1 equivalent of EtMgBr at –25 °C for 1 or 5 minutes resulted in a major species **1**, constituting 89-93% of iron in solution, with Mössbauer parameters δ = 0.68 mm/s and ΔE_Q = 1.89 mm/s (Figure 2 A, blue). The secondary species **2**, accounting for the remaining iron in solution, has Mössbauer parameters δ = 0.49 mm/s and ΔE_Q = 0.74 mm/s (Figure 2 A, red). Carrying out the analogous reaction with 2 equivalents of EtMgBr resulted in species **2** being the only iron species observed (Figure 2 B).

While the Mössbauer parameters and stoichiometric relationship suggested that **1** and **2** are the result of sequential transmetallation of the iron(II)-center, crystallization attempts were undertaken to confirm their identity. The relevant quantity of EtMgBr was added to a solution of $FeCl_2$ and 2 equivalents of TMEDA at –25 °C, followed by immediate cooling to –74 °C. Addition of hexane and leaving to stand at –80 °C for five days resulted in the formation of extremely air-, moisture- and temperature-sensitive colorless crystals suitable for single-crystal X-ray diffraction. These were identified as the mono- and bis-ethyl TMEDA-iron(II) complexes **1** and **2**, respectively. Both display distorted tetrahedral geometries with N-Fe-N angles of 82.24(12)º and 80.43(8)º, for **1** and **2** respectively (Figure 2 A and B, respectively). The iron-carbon bond lengths are 2.046(4) Å for **1** and 2.0821(15) Å for **2**; and the iron-nitrogen bond lengths 2.195(3) Å and 2.185 (3) for complex **1**, and 2.2437(15) Å for complex **2**. Additionally, **1** displays a halogen disorder with 70% bromide and 30% chloride occupancies. ^{57}Fe Mössbauer spectroscopy of crystalline material confirmed these to be the species generated *in situ*.

Addition of excess EtMgBr, including during catalytic reactions, did not result in the immediate displacement of TMEDA, with bis-ethyl complex **2** still observed as the major species (*vide infra*). This contrasts observations with mesitylmagnesium bromide by Bedford and co-workers, where addition of three or more equivalents of Grignard reagent resulted in displacement of TMEDA, even when present in excess.[29] As the alkyl moiety is expected to be a stronger σ-donor, it is likely that this difference in observed reactivity is dictated by steric factors.

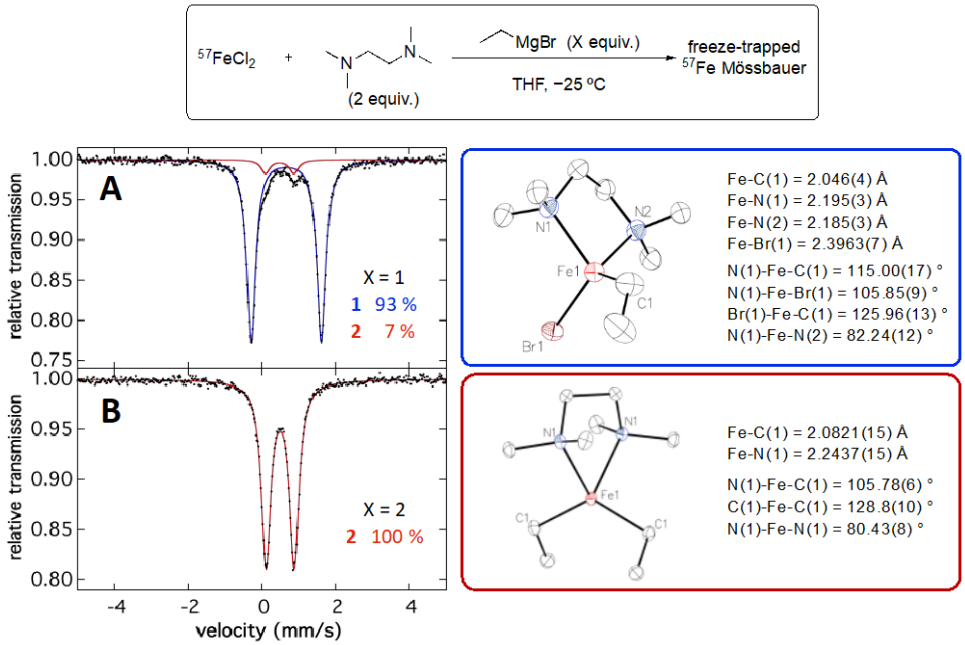

Figure 2. 80 K frozen solution Mössbauer spectra of the reaction of $^{57}FeCl_2$ with EtMgBr in the presence of 2 equiv. TMEDA and X-Ray crystal structures of major species formed with representative bond distances and angles. **A)** 1 equiv. EtMgBr, structure displays a halogen disorder with 70% bromide and 30% chloride occupancies; **B)** 2 equiv. EtMgBr. Note: Structure drawn with thermal displacement ellipsoids at 50% probability level. Iron shown in red, carbon in grey and hydrogen atoms omitted for clarity.

Alkyl-iron(II) complexes bearing β-hydrogens such as these are extremely rare, owing to their instability and propensity to undergo β-hydride elimination. To circumvent this, alkyl-iron(II) complexes have historically been prepared with these positions blocked. The most relevant example of this is the analogous high spin (S = 2) TMEDA-iron(II) bis-neopentyl complex, reported by Wolczanski and co-workers.[34] An alternative strategy has been to use strongly-stabilizing ligands which result in complexes resistant to β-hydride elimination.[35–41] Chelation of the alkyl ligand has also been demonstrated to make complexes resistant to β-hydride elimination. This was observed for N-heterocyclic carbene iron(II) complexes bearing (1,3-dioxan-2-yl)ethyl groups, with chelation through the carbon and one oxygen of the acetal group.[42] Other than complexes **1** and **2**, there are only two other examples of β-hydrogen-containing iron(II)-alkyl species without such stabilizing effects that have been isolated and characterized. These are a bisphosphine-iron(II) cyclohexyl complex reported by Fürstner and co-workers, with the bis-cyclohexyl analogue not isolated owing to its instability to further reaction,[35] and the partially reduced cluster $[Fe_8Et_{12}][MgX(THF)_5]_2$ reported by our group.[43] The scarcity of such β-hydrogen-containing alkyl-iron(II) complexes likely stems from their being short-lived intermediates preceding reduction to low oxidation-state iron species.[33,35,44,45] These include the formation of the formal iron(0) complex, $[BIPFe(Et)(CH_2{=}CH_2)]^-$, as well as bis-phosphine iron(0) ethene complexes, all of which result from reaction of the relevant ligand-supported iron(II) complex with EtMgBr.[33,35,46]

In Situ Evolution of Iron Speciation in the Presence of Styrene

In order to assess the potential further reaction of these alkyl-iron(II) complexes, and speciation under catalytically relevant conditions, freeze-trapped ^{57}Fe Mössbauer spectroscopy was carried out on similar reactions in the presence of styrene. A moderate excess of both EtMgBr and styrene (5 equiv.), as well as the temperature of –10 °C, were chosen in order to inhibit catalytic turnover and allow evaluation of the evolution of speciation. Five minutes after adding EtMgBr, TMEDA-iron(II) bis-alkyl complex **2** represented the major iron species in solution (Figure 3 A, red), together with two minor components **3** and **4** (Figure 3 A, grey and purple, respectively). With Mössbauer parameters δ = 0.19 mm/s and ΔE_Q = 1.53 mm/s, **3** initially represents 5% of iron in solution. The remaining 2% of iron in solution is **4**, with Mössbauer parameters δ = 0.36 mm/s and ΔE_Q = 1.35 mm/s. After 10 minutes only minor evolution in the speciation had taken place (see Supporting Information). The concentration of **3** remains constant, while **4** increases to 7% of iron in solution and **2** decreases correspondingly. However, after 30 and 60 minutes the speciation evolves more significantly. Although **2** remains the major species, it continues to decrease in concentration, eventually representing 40% of the iron in solution (Figure 3 B & C, red). Whereas **3** is no longer observed, the concentration of **4** increases, representing 23% of iron in solution after 30 minutes and 33% after 60 minutes (Figure 3, B & C, purple). After 30 minutes, a new species **5** is observed, with Mössbauer parameters δ = 0.44 mm/s and ΔE_Q = 0.88 mm/s. Initially representing 16% of iron in solution, **5** increases further to 27% after 60 minutes (Figure 3, B & C, orange). The initial presence and subsequent disappearance of **3** suggests that it reacts to form species **4** and/or **5**. This is consistent with subsequent experiments during catalysis, which indicate that **3** is an intermediate on the reduction pathway to the catalytically active species (*vide infra*).

Crystallization attempts were carried out adapting the above-described reaction. A solution of $FeCl_2$, 2 equivalents of TMEDA, and 5 equivalents of styrene was cooled to –25 °C before addition of 5 equivalents of EtMgBr. The solution was then cooled to –74 °C after which hexane was added, and the reaction left to stand

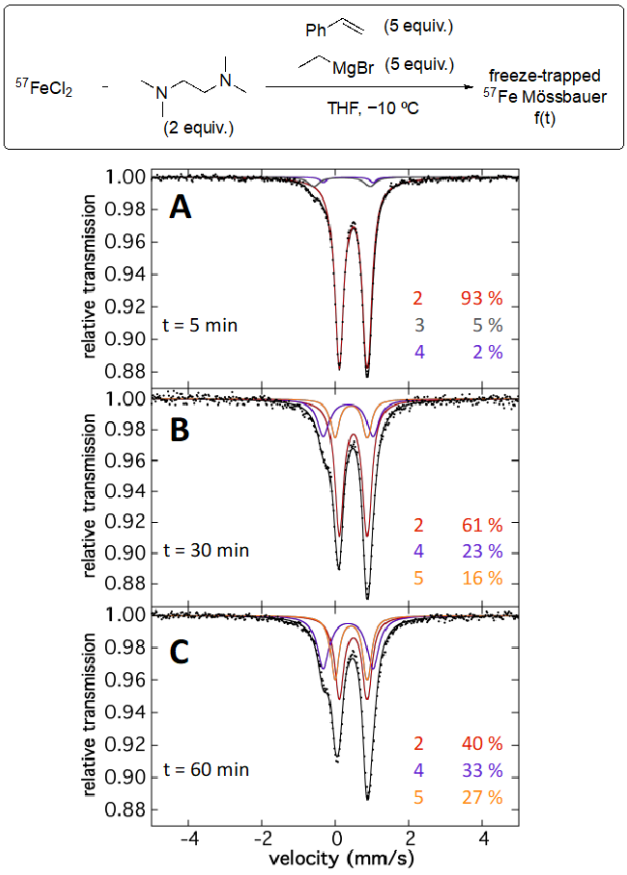

Figure 3. 80 K frozen-solution Mössbauer spectra of the reaction of $^{57}FeCl_2$ and 2 equiv. TMEDA with EtMgBr (5 equiv.) and styrene (5 equiv.) for A) 5 minutes; B) 30 minutes and C) 60 minutes.

overnight at –80 °C. This resulted in the formation of dark orange plates suitable for single-crystal X-ray diffraction. These highly air-, moisture- and temperature-sensitive crystals were identified as the tris-styrene-stabilized iron(0)-ethyl complex [Fe(η^2-styrene)$_3$(Et)][MgX(THF)$_5$] (Figure 4). ^{57}Fe Mössbauer spectroscopic parameters of isolated crystalline material were identical to the *in situ* formed **4**, confirming its identity. Reduction to form this styrene-stabilized iron(0)-ethyl complex **4**, in the presence of TMEDA, is in contrast to previous observations with bis-phosphine ligands by Fürstner and co-workers.[35] They observed that reaction of bis(diisopropylphosphino)propane-iron(II) dichloride with EtMgBr, in the presence of excess ethene, resulted in the iron(0) bis-ethene complex with the bis-phosphine ligand still bound. This may suggest that bis-phosphine ligands have a greater binding affinity to iron than TMEDA and are better able to stabilize the iron(0) center, avoiding dissociation in favor of styrene coordination. However, a higher binding affinity of styrene compared with ethene, due to greater π-backbonding, as well as increased sterics cannot be excluded as influences on the species formed.[47]

Having confirmed the identity of **4**, we next sought to identify the related species **5**. The reactivity studies above showed that **5** was present only once **4** had increased to significant concentrations. Along with their seemingly analogous rate of formation thereafter, this suggested that that **5** was somehow derived from **4**. The Mössbauer parameters of **5** also correspond precisely to those of the analogous tris-styrene ligated α-aryl-

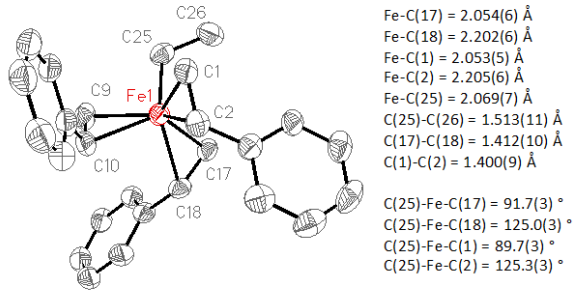

Figure 4. X-Ray crystal structure of [Fe(η^2-styrene)$_3$(Et)][MgX(THF)$_5$] **4** with representative bond distances and angles. Note: magnesium counter-cation omitted for clarity. Structure drawn with thermal displacement ellipsoids at 50% probability level. Iron shown in red, carbon in grey and hydrogen atoms omitted for clarity.

iron(0) complex [Fe(η^2-styrene)$_3$(κ^1-CH(CH$_3$)Ph)][MgX(THF)$_5$].[33] Further confirming this assignment was its crystallization from the reaction of Ph(CH$_2$)$_2$MgCl with $FeCl_2$ in the presence of 2 equivalents of TMEDA and 5 equivalents of styrene at –25 °C (Scheme 2). ^{57}Fe Mössbauer and ^{1}H-NMR spectroscopies of the dark red-black plates were also identical to those previously obtained. While the bond metrics are consistent with **4**, one notable difference is the longer iron-carbon bond of 2.150(4) Å, compared to 2.069(7) Å for **4**.

The previous identification of complex **5** was as a minor component in the bis(imino)pyridine iron-catalyzed hydromagnesiation reaction, resulting from displacement of the tridentate ligand.[33] While able to be isolated, **5** had to be prepared from the starting bis(imino)pyridine iron(II) dichloride complex as starting from $FeCl_2$ resulted in a complex mixture by ^{57}Fe Mössbauer spectroscopy. This demonstrates the significance of TMEDA in allowing controlled reduction to the styrene-stabilized iron(0) complexes through initial formation of a TMEDA-iron(II) bis-alkyl species such as **2**. Carrying out the analogous experiment to monitor the reduction of **2** in the presence of 5 equivalents of TMEDA, compared with 2 equivalents used previously, resulted in only TMEDA-iron(II) bis-alkyl complex **2** being observed even after 60 minutes (see Supporting Information). This observation that excess TMEDA inhibits the subsequent reduction of **2** to form **4** and **5**, suggests that this process proceeds by dissociation of TMEDA.

With the identities of both **4** and **5** established, a potential pathway for their associated formation becomes apparent. Net hydride transfer from the ethyl ligand to a bound styrene in complex **4**, followed by exchange of the resulting ethene for another equivalent of styrene would give **5**. As **5** effectively has an equivalent of product bound, turnover could be envisioned to take place by exchange with an equivalent of EtMgBr. This would release the product of hydromagnesiation, the α-aryl Grignard

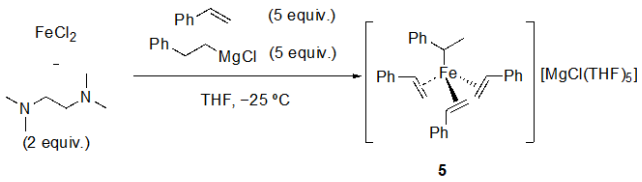

Scheme 2. Formation of **5** from the reaction of $FeCl_2$ with Ph(CH$_2$)$_2$MgCl in the presence of styrene and TMEDA.

reagent, and regenerate complex **4**. Overall, this now provides a more complete picture of how these iron(0) species are catalytically competent for the hydromagnesiation of styrene derivatives. Due to **5** previously being only a minor component, and having to be synthesized from the bis(imino)pyridine iron(II) complex, little had been established other than its effectiveness as a pre-catalyst.[33]

Table 1. Summary of 80 K Mössbauer parameters of isolated iron species.

	solid		frozen solution	
Complex	δ (mm/s)	ΔE_Q (mm/s)	δ (mm/s)	ΔE_Q (mm/s)
TMEDA$Fe^{II}EtBr$[a] **(1)**	0.67	1.82	0.68	1.89
TMEDA$Fe^{II}Et_2$ **(2)**	0.50	0.76	0.49	0.74
$(styrene)_3Fe^0$-Et **(4)**	0.37	1.37	0.36	1.35
$(styrene)_3Fe^0$-α-aryl **(5)**	0.44	0.88	0.44[b]	0.88[b]

[a] Structure displays halogen disorder with 70% bromide and 30% chloride occupancies [b] from reference 28.

Iron Speciation During Catalysis

Despite the competence of **5** as a pre-catalyst, as well as a reasonable reaction pathway involving **4** and **5** being evident, it was essential to establish whether these species are relevant and present in the catalytic reaction. The speciation during catalysis was assessed by freeze-trapped ^{57}Fe Mössbauer spectroscopy, carried out at various time-points during the hydromagnesiation of styrene using 3 mol% $^{57}FeCl_2$. In the presence of 1 equivalent of TMEDA, with respect to iron, 1 minute after adding EtMgBr (1.5 equiv.) catalytic turnover has already begun, with 12% product detected. At this time 77% of the iron in solution has already been reduced to the styrene-stabilized iron(0) complexes **4** and **5** (25% and 52%, respectively, see Supporting Information). Only a small portion (5%) of TMEDA-iron(II) bis-ethyl complex **2** was present, with the remaining iron consisting of the previously observed and transient species **3** (δ = 0.19 mm/s and ΔE_Q = 1.53 mm/s). Further into the reaction (5 minutes, 33% yield) **2** and **3** are no longer observed, while the combined concentrations of **4** and **5** have increased, with iron(0)-ethyl complex **4** now the major species at 64%. These results demonstrate that complexes **4** and **5** are indeed the catalytically active and major species present during catalytic hydromagnesiation using TMEDA. Furthermore, no significant EPR-active species were present *in situ* during catalysis (see Supporting Information).

In order to assess whether the observed stabilization of TMEDA-iron(II) bis-alkyl complex **2** in the presence of excess TMEDA would manifest under catalytic conditions, analogous freeze-trapped ^{57}Fe Mössbauer spectroscopy was carried out on the hydromagnesiation of styrene, this time with 5 equivalents of TMEDA with respect to iron. One minute after adding EtMgBr (1.5 equiv.), starkly different iron speciation is observed compared with the reaction using 1 equivalent of TMEDA. TMEDA-iron(II) bis-ethyl complex **2** was now observed to be the major iron species present in solution, at 88% (Figure 5 A, red). The remaining 12% of iron in solution is once again the transient species **3** (Figure 5 A, grey). Significantly, at this stage of the reaction no detectable product was observed. This indicates, perhaps unsurprisingly, that neither **2** or **3** are catalytically active and that the styrene-stabilized iron(0) complexes **4** and **5** are the catalytically relevant species. Further corroborating this is that after 5 minutes, catalytic turnover is occurring (21% yield) with **2** and **3** no longer present, while **4** and **5** together represent the majority of iron in solution at 86% (Figure 5 B, purple and orange, respectively). The remaining 14% of iron in solution is a previously unobserved species **6**, with Mössbauer parameters δ = 0.32 mm/s and ΔE_Q = 1.87 mm/s (Figure 5 B, green). As **6** was observed during catalytic turnover, the byproduct of which is ethene, it is possible that **6** is a related iron(0) complex differing by substitution of one or more equivalents of styrene for ethene. This is consistent with reports of the reaction protocol on a large scale requiring sparging with nitrogen, indicating that reversible binding of ethene takes place.[27]

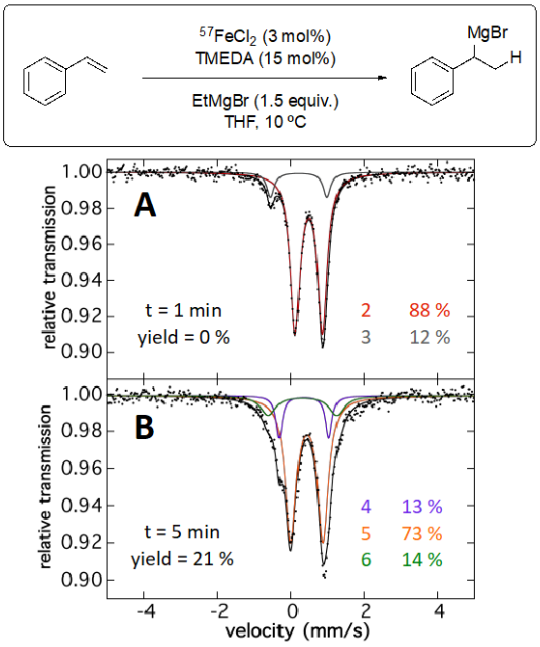

Figure 5. 80 K frozen solution Mössbauer spectra taken as a function of time during catalytic hydromagnesiation of styrene.

This once again demonstrates the degree to which excess TMEDA stabilizes **2**. The consequence of this stabilization is a significantly slower reduction of **2** to catalytically active **4** and **5**, as was also observed in the stoichiometric reactions. Slowing the rate of formation of the catalytically active species would in turn account for the significantly longer induction period observed when using larger excesses of TMEDA. This is further highlighted when compared to the catalytic reaction with 2 equivalents of TMEDA. In this case, after 1 minute, **4** and **5** are already the major iron species observed and catalysis occurring (*vide supra*). The more sustained catalytic activity also observed suggests TMEDA prevents catalyst deactivation by aggregation of the iron(0) species, which is consistent with the beneficial effects of TMEDA despite not being bound to the catalytically active species, **4** and **5**. Further supporting this is that iron nanoparticles, demonstrated to be active for hydrogenation, proved ineffective for the reaction.[48,49]

The transient species **3**, also observed during the induction period with excess TMEDA, displayed similar Mössbauer parameters (δ = 0.19 mm/s and ΔE_Q = 1.53 mm/s) to a previously identified iron(II) tri-ethyl ferrate complex (δ = 0.19 mm/s and ΔE_Q = 1.43 mm/s).[43] As the tri-ethyl ferrate species was demonstrated to have a distinctive near-infrared magnetic circular dichroism (NIR MCD) spectrum, this was used to probe whether this was the identity of **3**. Carrying out the analogous catalytic reaction in 1:1.5 THF/2-MeTHF, for glassing purposes, MCD samples were frozen in liquid nitrogen after 1 minute. It should be noted that ^{57}Fe Mössbauer spectroscopy showed that the iron speciation was not affected by this solvent mixture. The 5 K NIR MCD spectrum showed two intense transitions at ≈ 5940 cm^{-1} and ≈ 6900 cm^{-1}, corresponding to TMEDA-iron(II) bis-ethyl complex **2** (see Supporting Information). Transitions corresponding to the tri-ethyl ferrate complex (≈ 9200 cm^{-1} and ≈ 10200 cm^{-1}) were not observed, although an additional transition was observed at ≈ 12300 cm^{-1}. While this rules out the presence of the tri-ethyl ferrate complex, a similar spectral feature resulting from decomposition was observed as a minor component.[43] This potentially arises from a similar reduction process through β-hydride elimination, forming a reduced species related to the transient intermediate **3**. Consistent with these species being related is the fact that the stoichiometric reactivity indicates that reduction of **2** is dissociative with respect to TMEDA, after which a species similar to the tri-ethyl ferrate could form. The resulting species, **3** in the case of hydromagnesiation reaction conditions, subsequently reacts further in the presence of styrene to form the styrene-stabilized iron(0) complexes observed. However, due to it being observed in only relatively small amounts along with its transient nature, the unambiguous assignment of **3** remains elusive.

Conclusion

The use of ^{57}Fe Mössbauer spectroscopy to monitor *in situ* iron speciation and guide the isolation of key reactive intermediates in the iron-catalyzed hydromagnesiation of styrene derivatives with TMEDA. This study also revealed the multifaceted nature of the influence TMEDA exerts on both speciation and reactivity. Initial coordination of TMEDA to the iron center results in formation of iron(II) mono- and bis-ethyl complexes. Formation of the TMEDA-iron(II) bis-alkyl complex is key, as it undergoes selective reduction to form the catalytically active styrene-stabilized iron(0) complexes. Despite not being coordinated to the catalytically active species, TMEDA is essential to its selective formation. Additionally, the quantity of TMEDA present influences the rate of this reduction process. Beyond this, TMEDA also aids in preventing catalyst deactivation, which likely occurs through aggregation of the active iron(0) species. This manifests in more sustained catalytic performance.

The role of TMEDA in allowing controlled reduction represents a new paradigm in iron catalysis for this long-established and versatile additive, as well as demonstrating multiple ways in which it can exert beneficial effects even in a single catalytic reaction. As TMEDA a crucial additive in various iron-catalyzed reactions, the implications of this study extend beyond hydromagnesiation. For example, despite not being on-cycle active species for the hydromagnesiation reaction, the TMEDA-iron(II) alkyl complexes represent potential intermediates in the cross-coupling of alkyl Grignard reagents with aryl chlorides and will be the subject of future work.[20]

Acknowledgements

This work was supported by a grant from the National Institutes of Health (R01GM111480 to M.L.N.). S.P.T. thanks the Royal Society for a University Research Fellowship. The NSF is gratefully acknowledged for support for the acquisition of an X-ray diffractometer (CHE-1725028).

Deposition numbers 2002512-2002514 contain the supplementary crystallographic data for this paper. These data are provided free of charge by the joint Cambridge Crystallographic Data Centre and Fachinformationszentrum Karlsruhe Access Structures service www.ccdc.cam.ac.uk/structures.

Keywords: iron • catalysis • hydromagnesiation • TMEDA • mechanism

[1] B. D. Sherry, A. Fürstner, *Acc. Chem. Res.* **2008**, *41*, 1500–1511.

[2] E. Nakamura, N. Yoshikai, *J. Org. Chem.* **2010**, *75*, 6061–6067.

[3] I. Bauer, H.-J. Knoelker, *Chem. Rev.* **2015**, *115*, 3170–3387.

[4] A. Fürstner, *ACS Cent. Sci.* **2016**, *2*, 778–789.

[5] E. Bauer, Ed. , *Iron Catalysis II*, Springer International Publishing, **2015**.

[6] A. Piontek, E. Bisz, M. Szostak, *Angew. Chemie Int. Ed.* **2018**, *57*, 11116–11128.

[7] M. D. Greenhalgh, A. S. Jones, S. P. Thomas, *ChemCatChem* **2014**, *7*, 190–222.

[8] P. J. Chirik, *Angew. Chemie Int. Ed.* **2017**, *56*, 5170–5181.

[9] J. V Obligacion, P. J. Chirik, *Nat. Rev. Chem.* **2018**, *2*, 15–34.

[10] R. Shang, L. Ilies, E. Nakamura, *Chem. Rev.* **2017**, *117*, 9086–9139.

[11] P. Gandeepan, T. Müller, D. Zell, G. Cera, S. Warratz, L. Ackermann, *Chem. Rev.* **2019**, *119*, 2192–2452.

[12] J. Loup, U. Dhawa, F. Pesciaioli, J. Wencel-Delord, L. Ackermann, *Angew. Chemie Int. Ed.* **2019**, *58*, 12803–12818.

[13] M. Nakamura, K. Matsuo, S. Ito, E. Nakamura, *J. Am. Chem. Soc.* **2004**, *126*, 3686–3687.

[14] R. B. Bedford, D. W. Bruce, R. M. Frost, M. Hird, *Chem. Commun.* **2005**, 4161–4163.

[15] G. Cahiez, V. Habiak, C. Duplais, A. Moyeux, *Angew. Chemie Int. Ed.* **2007**, *46*, 4364–4366.

[16] A. Guérinot, S. Reymond, J. Cossy, *Angew. Chemie Int. Ed.* **2007**, *46*, 6521–6524.

[17] W. M. Czaplik, M. Mayer, A. Jacobi von Wangelin, *Angew. Chemie Int. Ed.* **2009**, *48*, 607–610.

[18] W. M. Czaplik, M. Mayer, A. Jacobi von Wangelin, *ChemCatChem* **2011**, *3*, 135–138.

[19] S. E. Denmark, A. J. Cresswell, *J. Org. Chem.* **2013**, *78*, 12593–12628.

[20] P. J. Rushworth, D. G. Hulcoop, D. J. Fox, *J. Org. Chem.* **2013**, *78*, 9517–9521.

[21] Z. Jia, Q. Liu, X.-S. Peng, H. N. C. Wong, *Nat. Commun.* **2016**, *7*, 10614.

[22] W. Miao, Y. Zhao, C. Ni, B. Gao, W. Zhang, J. Hu, *J. Am. Chem. Soc.* **2018**, *140*, 880–883.

[23] T. C. Atack, R. M. Lecker, S. P. Cook, *J. Am. Chem. Soc.* **2014**, *136*, 9521–9523.

[24] M. Y. Wong, T. Yamakawa, N. Yoshikai, *Org. Lett.* **2015**, *17*, 442–445.

[25] J. Loup, D. Zell, J. C. A. Oliveira, H. Keil, D. Stalke, L. Ackermann, *Angew. Chemie Int. Ed.* **2017**, *56*, 14197–14201.

[26] A. S. Jones, J. F. Paliga, M. D. Greenhalgh, J. M. Quibell, A. Steven, S. P. Thomas, *Org. Lett.* **2014**, *16*, 5964–5967.

[27] M. D. Greenhalgh, A. Kolodziej, F. Sinclair, S. P. Thomas, *Organometallics* **2014**, *33*, 5811–5819.

[28] D. Noda, Y. Sunada, T. Hatakeyama, M. Nakamura, H. Nagashima, *J. Am. Chem. Soc.* **2009**, *131*, 6078–6079.

[29] R. B. Bedford, P. B. Brenner, E. Carter, P. M. Cogswell, M. F. Haddow, J. N. Harvey, D. M. Murphy, J. Nunn, C. H. Woodall, *Angew. Chemie Int. Ed.* **2014**, *53*, 1804–1808.

[30] R. B. Bedford, P. B. Brenner, D. Elorriaga, J. N. Harvey, J. Nunn, *Dalt. Trans.* **2016**, *45*, 15811–15817.

[31] R. B. Bedford, *Acc. Chem. Res.* **2015**, *48*, 1485–1493.

[32] M. D. Greenhalgh, S. P. Thomas, *J. Am. Chem. Soc.* **2012**, *134*, 11900–11903.

[33] P. G. N. Neate, M. D. Greenhalgh, W. W. Brennessel, S. P. Thomas, M. L. Neidig, *J. Am. Chem. Soc.* **2019**, *141*, 10099–10108.

[34] B. P. Jacobs, P. T. Wolczanski, Q. Jiang, T. R. Cundari, S. N. MacMillan, *J. Am. Chem. Soc.* **2017**, *139*, 12145–12148.

[35] A. Casitas, H. Krause, R. Goddard, A. Fürstner, *Angew. Chemie Int. Ed.* **2015**, *54*, 1521–1526.

[36] N. Shirasawa, M. Akita, S. Hikichi, Y. Moro-oka, *Chem. Commun.* **1999**, 417–418.

[37] F. A. Jové, C. Pariya, M. Scoblete, G. P. A. Yap, K. H. Theopold, *Chem. – A Eur. J.* **2011**, *17*, 1310–1318.

[38] J. Vela, J. M. Smith, R. J. Lachicotte, P. L. Holland, *Chem. Commun.* **2002**, 2886–2887.

[39] J. Vela, S. Vaddadi, T. R. Cundari, J. M. Smith, E. A. Gregory, R. J. Lachicotte, C. J. Flaschenriem, P. L. Holland, *Organometallics* **2004**, *23*, 5226–5239.

[40] S. M. Bellows, T. R. Cundari, P. L. Holland, *Organometallics* **2013**, *32*, 4741–4751.

[41] J. M. Smith, R. J. Lachicotte, P. L. Holland, *Organometallics* **2002**, *21*, 4808–4814.

[42] V. E. Fleischauer, S. B. Muñoz III, P. G. N. Neate, W. W. Brennessel, M. L. Neidig, *Chem. Sci.* **2018**, *9*, 1878–1891.

[43] J. D. Sears, S. B. Muñoz, S. L. Daifuku, A. A. Shaps, S. H. Carpenter, W. W. Brennessel, M. L. Neidig, *Angew. Chemie Int. Ed.* **2019**, *58*, 2769–2773.

[44] M. D. Greenhalgh, D. J. Frank, S. P. Thomas, *Adv. Synth. Catal.* **2014**, *356*, 584–590.

[45] M. D. Greenhalgh, S. P. Thomas, *Chem. Commun.* **2013**, *49*, 11230–11232.

[46] A. Casitas, H. Krause, S. Lutz, R. Goddard, E. Bill, A. Fürstner, *Organometallics* **2018**, *37*, 729–739.

[47] Y. Yu, J. M. Smith, C. J. Flaschenriem, P. L. Holland, *Inorg. Chem.* **2006**, *45*, 5742–5751.

[48] P.-H. Phua, L. Lefort, J. A. F. Boogers, M. Tristany, J. G. de Vries, *Chem. Commun.* **2009**, 3747–3749.

[49] A. Welther, M. Bauer, M. Mayer, A. Jacobi von Wangelin, *ChemCatChem* **2012**, *4*, 1088–1093.

Entry for the Table of Contents

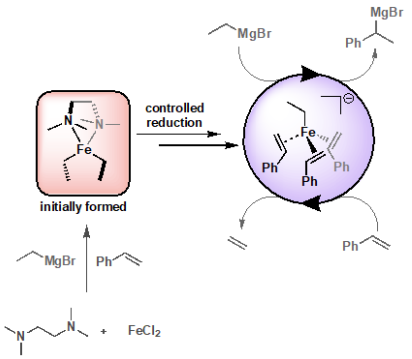

Studying the iron-catalyzed hydromagnesiation of styrene derivatives using TMEDA identified initial formation of TMEDA-iron(II) alkyl species. These undergo controlled reduction to selectively form catalytically active styrene-stabilized iron(0)-alkyl complexes not accessible in the absence of TMEDA. This controlled reduction and access to iron(0) species represents a new paradigm for the role of TMEDA as an additive in iron catalysis.